Journal of Materials Science Research; Vol. 2, No. 3; 2013
ISSN 1927-0585 E-ISSN 1927-0593
Published by Canadian Center of Science and Education

Combustion of Toluene Catalyzed by $Pt/Co_3O_4/CeO_2$-ZrO_2-SnO_2/γ-Al_2O_3

Min Yeong Kim[1], Tomoya Kamata[1], Toshiyuki Masui[1] & Nobuhito Imanaka[1]

[1] Department of Applied Chemistry, Faculty of Engineering, Osaka University, Osaka, Japan

Correspondence: Nobuhito Imanaka, Department of Applied Chemistry, Faculty of Engineering, Osaka University, 2-1 Yamadaoka, Suita, Osaka 565-0871, Japan. Tel: 81-6-6879-7352. Fax: 81-6-6879-7354. E-mail: imanaka@chem.eng.osaka-u.ac.jp

Received: February 4, 2013 Accepted: April 6, 2013 Online Published: April 15, 2013

doi:10.5539/jmsr.v2n3p51 URL: http://dx.doi.org/10.5539/jmsr.v2n3p51

Abstract

A 1wt%$Pt/Co_3O_4/CeO_2$-ZrO_2-SnO_2/γ-Al_2O_3 catalyst was prepared to realize complete combustion of toluene at the lowest temperature possible without excessive use of platinum particles. The addition of Co_3O_4 to Pt/CeO_2-ZrO_2-SnO_2/γ-Al_2O_3 as a promoter was effective in decreasing the amount of platinum without significant reduction in the catalytic activity. The highest activity for the combustion of toluene was observed using the 1wt%Pt/11wt%Co_3O_4/16wt%$Ce_{0.62}Zr_{0.20}Sn_{0.18}O_{2.0}/\gamma$-$Al_2O_3$ catalyst, and despite a smaller platinum loading in the present catalyst, toluene was completely oxidized to carbon dioxide and water vapor at a lower temperature of 160 ^{o}C compared to that using 5wt%Pt/γ-Al_2O_3 at 170 ^{o}C.

Keywords: volatile organic compounds, catalytic combustion, toluene, oxidation, rare earth oxide

1. Introduction

Some examples of volatile organic compounds (VOCs) are aldehydes, ketones, and other light weight hydrocarbons. Since they have relatively high vapor pressures under ambient conditions, they vaporize and diffuse easily into the atmosphere. Some VOCs are harmful to human health and the environment. They have been known to cause sick building syndrome, multiple chemical sensitivity, and air pollution such as photo-chemical smog and ground-level ozone (Atkinson et al., 2003; Ryerson et al., 2001).

Among the VOCs, toluene is widely used as an organic solvent for paints, printing inks, adhesives, and antiseptics due to its excellent ability to dissolve organic substances. Conseuently, in order to avoid the above-mentioned harmful effects, it is necessary to reduce the amount of toluene released into the atmosphere as much as possible.

For effective reduction, several methods have been proposed such as catalytic combustion (Sungkono et al., 1997), flame combustion (Hamins et al., 1987), catalytic decomposition using ozone and plasma (Harling et al., 2009), photocatalytic decomposition (Einaga et al., 2002), and the adsorbent-based method (Hauxell et al., 1968). Among these methods, complete catalytic combustion of toluene into carbon dioxide and water vapor at moderate temperatures is an ecologically simple and clean technology to eliminate toluene (Spivey, 1987). A number of combustion catalysts for the reduction of toluene have been reported. However, it is difficult to accomplish complete combustion of toluene at low temperatures. Moreover, the catalyst needs to be heated to at least 200 °C (Imanaka et al., 2011; Saqer et al., 2009).

On the contrary, in our previous studies, we found that a combination of platinum and a solid that can supply reactive oxygen molecules below 100 °C (Imanaka et al., 2005, 2007, 2011; Masui et al., 2006, 2007; Minami et al., 2006) was significantly effective in inducing the oxidation of VOCs by oxygen pullover from $Ce_{0.64}Zr_{0.16}Bi_{0.20}O_{1.90}/\gamma$-$Al_2O_3$ to platinum nanoparticles (Imanaka et al., 2008, 2009). In fact, we found that a 7wt%Pt/16wt%$Ce_{0.64}Zr_{0.16}Bi_{0.20}O_{1.90}/\gamma$-$Al_2O_3$ catalyst can completely oxidize toluene at 120 °C (Masui et al., 2010). Furthermore, we demonstrated in our recent study that a 10wt%Pt/16wt%$Ce_{0.68}Zr_{0.17}Sn_{0.15}O_{2.0}/\gamma$-$Al_2O_3$ catalyst can completely oxidize toluene at a temperature as low as 110 °C (Yasuda et al., 2012). However, a relatively large amount of platinum was supported on these catalysts, leading to high cost production from a practical application standpoint. Therefore, it is necessary to reduce the precious metal content in the catalysts as much as possible with no significant decrease in the catalytic activity.

To realize such advanced catalysts, we focused on cobalt oxide (Co_3O_4) as a promoter to facilitate the oxidation of toluene without excessive use of platinum, since Co_3O_4 was reported to have the highest catalytic activity for VOCs oxidation among several transition metal oxides investigated (Chianelli et al., 2009; Lamonier et al., 2007; Liotta et al., 2009; Pedrosa et al., 2003; Rybak et al., 2011; Wyrwalski et al., 2010). In this study, the amount of platinum was decreased to 1wt% and Co_3O_4 was employed as a promoter: 1wt%Pt/11wt%Co_3O_4/16wt% CeO_2-ZrO_2-SnO_2/γ-Al_2O_3 catalysts were prepared and the effect of Co_3O_4 on the activity of toluene oxidation was investigated. Furthermore, the catalyst composition was optimized to give the highest activity.

2. Experimental

A $Ce_{0.62}Zr_{0.20}Sn_{0.18}O_{2.0}$/γ-$Al_2O_3$ support was synthesized by co-precipitation and impregnation methods: the $Ce_{0.62}Zr_{0.20}Sn_{0.18}O_{2.0}$ was synthesized by co-precipitation and the subsequent deposition on γ-Al_2O_3 was carried out by impregnation. SnC_2O_4 was dissolved in a mixture of 1.0 mol L^{-1} $Ce(NO_3)_3$ and 0.1 mol L^{-1} $ZrO(NO_3)_2$ aqueous solutions in a stoichiometric ratio, and then the mixture was impregnated on commercially available γ-Al_2O_3 (DK Fine, AA-300). The $Ce_{0.62}Zr_{0.20}Sn_{0.18}O_{2.0}$ content was adjusted to 16wt% of the total support to optimize the oxygen release ability (Yasuda et al., 2012). The pH of the aqueous mixture was adjusted to 11 by dropwise addition of aqueous ammonia (5%), whereby the $Ce_{0.62}Zr_{0.20}Sn_{0.18}O_{2.0}$ particles were precipitated on the surface of γ-Al_2O_3. After stirring for 12 h at room temperature, the resulting $Ce_{0.62}Zr_{0.20}Sn_{0.18}O_{2.0}$/γ-$Al_2O_3$ support was collected by filtration, washed several times with deionized water, and then dried at 80 °C for 6 h. The sample was ground in an agate mortar and calcined at 600 °C for 1 h in an ambient atmosphere.

Supported cobalt oxide catalysts [*x*wt%Co_3O_4/16wt%$Ce_{0.62}Zr_{0.20}Sn_{0.18}O_{2.0}$/γ-$Al_2O_3$ (x = 7, 11, and 14)] were prepared by mixing a 0.1 mol L^{-1} $Co(NO_3)_3$ aqueous solution with the $Ce_{0.62}Zr_{0.20}Sn_{0.18}O_{2.0}$/γ-$Al_2O_3$ support. After mixing, the homogeneous samples were evaporated to dryness at 80 °C for 12 h, and then calcined at 500 °C for 1 h in an ambient atmosphere.

A supported platinum catalyst (1wt%Pt/xwt%Co_3O_4/16wt%$Ce_{0.62}Zr_{0.20}Sn_{0.18}O_{2.0}$/γ-$Al_2O_3$) was prepared by impregnating the *x*wt%Co_3O_4/16wt%$Ce_{0.62}Zr_{0.20}Sn_{0.18}O_{2.0}$/γ-$Al_2O_3$ support, in which the amount of Co_3O_4(x) was optimized to give the highest activity, with a 4wt% platinum colloid stabilized with polyvinylpyrrolidone in a water solvent (Tanaka Kikinzoku Kogyo Co., Ltd.). After impregnation, the sample was dried at 80 °C for 12 h, and then calcined at 450 °C or 500 °C for 4 h. For references, a 1wt%Pt/16wt%$Ce_{0.68}Zr_{0.17}Sn_{0.15}O_{2.0}$/γ-$Al_2O_3$ catalyst without Co_3O_4 and a 5wt%Pt/γ-Al_2O_3 catalyst were also prepared using the same procedure.

The sample compositions were analyzed using an X-ray fluorescence spectrometer (XRF; Rigaku, ZSX-100e). The crystal structures of the catalysts were identified by X-ray powder diffraction (XRD; Rigaku, SmartLab) using Cu-Kα radiation (40 kV, 30 mA). The Brunauer-Emmett-Teller (BET) specific surface area was measured by nitrogen adsorption at −196 °C and pore size distribution (PSD) plots were obtained by Barrett–Joyner–Halenda (BJH) method using the cylindrical pore model (Micromeritics Tristar 3000). X-ray photoelectron spectroscopy (XPS; ULVAC 5500MT) measurement was performed at room temperature using Mg-Kα radiation (1253.6 eV). The effect of charging on the binding energies was corrected with respect to the C 1s peak at 284.6 eV. Transmission electron microscopic images were also taken with an accelerating voltage of 200 kV (TEM; Hitachi H-800). Temperature programmed reduction (TPR) measurements were carried out under a flow of pure H_2 (80 mL min^{-1}) at a heating rate of 5 K min^{-1} using a gas chromatograph with a thermal conductivity detector (TCD; Shimadzu GC-8AIT). Following the TPR experiments, the total oxygen storage capacity (OSC) was measured using a pulse-injection method at 427 °C (700 K).

The oxidation activity for toluene was tested in a conventional fixed-bed flow reactor consisting of a 10-mm-diameter quartz glass tube. The feed gas was composed of 0.09 vol% toluene in an air balance and the rate was 20 mL min^{-1} over 0.1 g of the catalyst [space velocity (S.V.) = 12,000 L kg^{-1} h^{-1}]. Prior to the measurements, the catalyst was heated at 200 °C for 2 h in a flow of Ar (20 mL min^{-1}) to remove water molecules adsorbed on the surface of the catalyst. The catalytic activity was evaluated in terms of toluene conversion. The gas composition after the reaction was analyzed using a gas chromatograph with a flame ionization detector (FID; Shimadzu GC-8AIF) and a gas chromatograph-mass spectrometer (GC-Mass; Shimadzu GCMS-QP2010 Plus).

3. Results and Discussion

Figure 1 shows XRD patterns of the 16wt%$Ce_{0.62}Zr_{0.20}Sn_{0.18}O_{2.0}$/γ-$Al_2O_3$ (CZS/Al_2O_3), 7wt%Co_3O_4/16wt% $Ce_{0.62}Zr_{0.20}Sn_{0.18}O_{2.0}$/γ-$Al_2O_3$ (7Co/CZS/Al_2O_3), 11wt%Co_3O_4/16wt%$Ce_{0.62}Zr_{0.20}Sn_{0.18}O_{2.0}$/γ-$Al_2O_3$ (11Co/CZS/ Al_2O_3), and 15wt%Co_3O_4/16wt%$Ce_{0.62}Zr_{0.20}Sn_{0.18}O_{2.0}$/γ-$Al_2O_3$ (15Co/CZS/Al_2O_3) catalysts. The XRD results for the CZS/Al_2O_3 support show only peaks corresponding to the cubic fluorite-type oxide, Co_3O_4, and γ-Al_2O_3, and no crystalline impurities were observed. The diffraction peaks assigned to the cubic fluorite type structure were

steady and no peak shift was observed regardless of the amount of cobalt oxide, indicating that Co_3O_4 was supported on the surface of the CZS/Al_2O_3 support without forming solid solutions with CZS or γ-Al_2O_3.

BET specific surface areas of the CZS/Al_2O_3, 7Co/CZS/Al_2O_3, 11Co/CZS/Al_2O_3, and 15Co/CZS/Al_2O_3 catalysts are summarized in Table 1. The BET specific surface areas of the cobalt-supported catalysts were smaller than that of CZS/Al_2O_3, and they decreased with increasing Co_3O_4 content. These results suggest that some of the Co_3O_4 particles are supported in the pores of CZS/Al_2O_3.

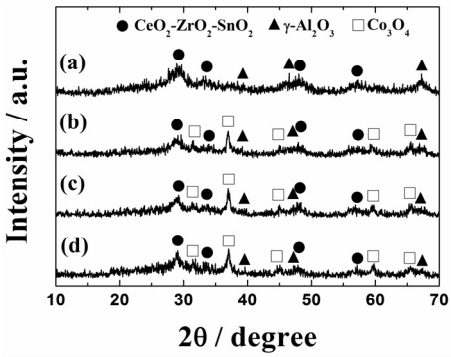

Figure 1. XRD patterns of the (a) 16wt%$Ce_{0.62}Zr_{0.20}Sn_{0.18}O_{2.0}$/γ-$Al_2O_3$, (b) 7wt%$Co_3O_4$/16wt%$Ce_{0.62}Zr_{0.20}Sn_{0.18}O_{2.0}$/γ-$Al_2O_3$, (c) 11wt%$Co_3O_4$/16wt%$Ce_{0.62}Zr_{0.20}Sn_{0.18}O_{2.0}$/γ-$Al_2O_3$, and (d) 15wt%$Co_3O_4$/16wt%$Ce_{0.62}Zr_{0.20}Sn_{0.18}O_{2.0}$/γ-$Al_2O_3$ catalysts (●:CeO_2-ZrO_2-SnO_2, ▲:γ-Al_2O_3, □:Co_3O_4)

Table 1. Composition and BET surface area of the catalysts

Catalyst	Catalyst composition	BET surface area (m^2 g^{-1})
CZS/Al_2O_3	16wt%$Ce_{0.62}Zr_{0.20}Sn_{0.18}O_{2.0}$/γ-$Al_2O_3$	190
7Co/CZS/Al_2O_3	7wt%Co_3O_4/16wt%$Ce_{0.62}Zr_{0.20}Sn_{0.18}O_{2.0}$/γ-$Al_2O_3$	151
11Co/CZS/Al_2O_3	11wt%Co_3O_4/16wt%$Ce_{0.62}Zr_{0.20}Sn_{0.18}O_{2.0}$/γ-$Al_2O_3$	141
15Co/CZS/Al_2O_3	15wt%Co_3O_4/16wt%$Ce_{0.62}Zr_{0.20}Sn_{0.18}O_{2.0}$/γ-$Al_2O_3$	139
1Pt/11Co/Al_2O_3	1wt%Pt/11wt%Co_3O_4/γ-Al_2O_3	166
1Pt/CZS/Al_2O_3	1wt%Pt/16wt%$Ce_{0.62}Zr_{0.20}Sn_{0.18}O_{2.0}$/γ-$Al_2O_3$	176
1Pt/11Co/CZS/Al_2O_3	1wt%Pt/11wt%Co_3O_4/16wt%$Ce_{0.62}Zr_{0.20}Sn_{0.18}O_{2.0}$/γ-$Al_2O_3$	131

Figure 2 depicts temperature dependencies of toluene oxidation over the 7Co/CZS/Al_2O_3, 11Co/CZS/Al_2O_3, and 15Co/CZS/Al_2O_3 catalysts. Toluene was completely oxidized into CO_2 and water vapor, and no CO and toluene-derived compounds were detected as by-products with a gas chromatograph. The toluene oxidation activity depends on the catalyst composition, and the highest activity was obtained for 11Co/CZS/Al_2O_3. However, the activity decreased with increasing Co_3O_4 content beyond the optimum amount, probably due to Co_3O_4 agglomeration and particle growth. Toluene oxidation activity of the optimum 11Co/CZS/Al_2O_3 catalyst was initially observed at 100 °C, and complete oxidation of toluene was confirmed at 300 °C. Unfortunately, this temperature was higher than that of 10wt%Pt/16wt%$Ce_{0.68}Zr_{0.17}Sn_{0.15}O_{2.00}$/γ-$Al_2O_3$ (110 °C) previously reported by our group (Yasuda et al., 2012). Therefore, to increase the catalytic activity of 11Co/CZS/Al_2O_3, a small amount of platinum (1wt%) was additionally supported on the surface of the catalyst.

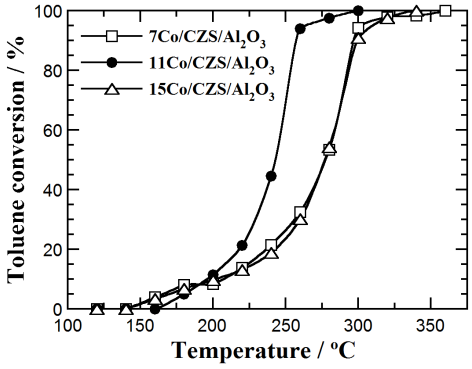

Figure 2. Temperature dependencies of toluene oxidation on the (a) 7wt%Co_3O_4/16wt%$Ce_{0.62}Zr_{0.20}Sn_{0.18}O_{2.0}$/γ-$Al_2O_3$, (b) 11wt%$Co_3O_4$/16wt%$Ce_{0.62}Zr_{0.20}Sn_{0.18}O_{2.0}$/γ-$Al_2O_3$, and (c) 15wt%$Co_3O_4$/16wt%$Ce_{0.62}Zr_{0.20}Sn_{0.18}O_{2.0}$ /γ-Al_2O_3 catalysts

Figure 3 shows XRD patterns of 1wt%Pt/11wt%Co_3O_4/16wt%$Ce_{0.62}Zr_{0.20}Sn_{0.18}O_{2.00}$/γ-$Al_2O_3$ (1Pt/11Co/CZS/Al_2O_3) and 1wt%Pt/16wt%$Ce_{0.62}Zr_{0.20}Sn_{0.18}O_{2.00}$/γ-$Al_2O_3$ (1Pt/CZS/Al_2O_3). In addition, in these cases, only $Ce_{0.62}Zr_{0.20}Sn_{0.18}O_{2.00}$, Co_3O_4, and γ-Al_2O_3 were observed in the XRD patterns and no peaks corresponding to platinum appeared probably due to the small platinum particles that are highly dispersed on the surface of the catalysts.

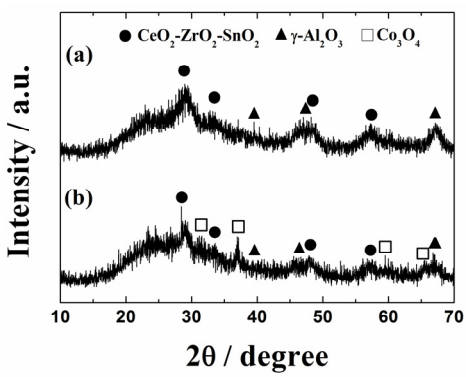

Figure 3. XRD patterns of the (a) 1wt%Pt/16wt%$Ce_{0.62}Zr_{0.20}Sn_{0.18}O_{2.0}$/γ-$Al_2O_3$ and (b) 1wt%Pt/11wt%Co_3O_4 /16wt%$Ce_{0.62}Zr_{0.20}Sn_{0.18}O_{2.0}$/γ-$Al_2O_3$ catalysts (●:CeO_2-ZrO_2-SnO_2, ▲:γ-Al_2O_3, □:Co_3O_4)

The bright and dark field TEM images of 1Pt/11Co/CZS/Al_2O_3 and 1Pt/CZS/Al_2O_3 are depicted in Figure 4. As shown by these photographs, there is no clear difference in the size and dispersion state of platinum particles in these catalysts, which are recognized as bright spots in the dark field images in Figures 4(b) and (d). The particle size of platinum was estimated using these spots and it was confirmed to be smaller than 5 nm for both catalysts. Furthermore, it is also found that Co_3O_4 is present as needle crystals by comparing the bright field image of 1Pt/11Co/CZS/Al_2O_3 with that of 1Pt/CZS/Al_2O_3. BET specific surface areas of 1Pt/CZS/Al_2O_3 and 1Pt/11Co/CZS/Al_2O_3 are also listed in Table 1. The surface area of the latter is smaller than that of the former, which might be as a result of the Co_3O_4 deposition in the pore of CZS/Al_2O_3, as mentioned above.

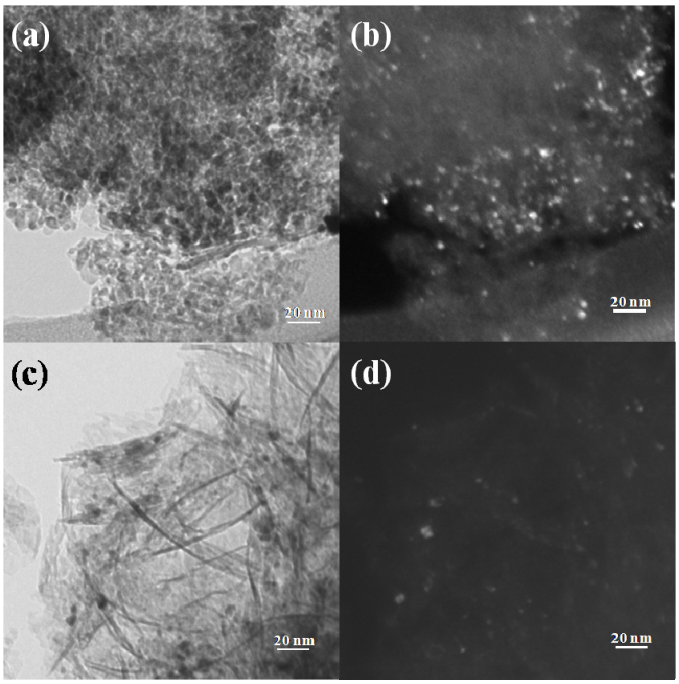

Figure 4. Transmission electron micrographs (TEM) of the (a), (b) 1wt%Pt/16wt%$Ce_{0.62}Zr_{0.20}Sn_{0.18}O_{2.0}$/γ-$Al_2O_3$, and (c), (d) 1wt%Pt/11wt%Co_3O_4/16wt%$Ce_{0.62}Zr_{0.20}Sn_{0.18}O_{2.0}$/γ-$Al_2O_3$ catalysts: (a), (c) are bright field images, and (b), (d) are dark field images

The BJH desorption pore size distribution plots of 1Pt/CZS/Al_2O_3 and 1Pt/11Co/CZS/Al_2O_3 are shown in Figure 5. As evidenced in this figure, these catalyst particles have a narrow mesopore size distribution at 6 nm and the size was maintained even if Co_3O_4 was deposited on $Ce_{0.62}Zr_{0.20}Sn_{0.18}O_{2.0}$/γ-$Al_2O_3$. However, the pore volume was significantly decreased by the Co_3O_4 deposition, which supports the above discussion.

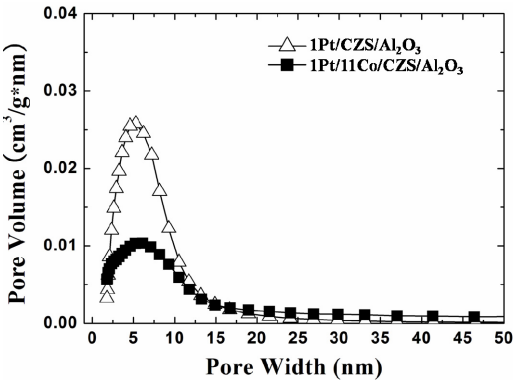

Figure 5. BJH pore distribution plots of the 1wt%Pt/16wt%$Ce_{0.62}Zr_{0.20}Sn_{0.18}O_{2.0}$/γ-$Al_2O_3$ and 1wt%Pt/11wt%Co_3O_4/16wt%$Ce_{0.62}Zr_{0.20}Sn_{0.18}O_{2.0}$/γ-$Al_2O_3$ catalysts.

Figure 6 shows the temperature dependencies of toluene oxidation over the 1Pt/11Co/CZS/Al_2O_3 and 11Co/CZS/Al_2O_3 catalysts. Results for 1Pt/CZS/Al_2O_3, 1Pt/11Co/Al_2O_3, and conventional 5wt%Pt/γ-Al_2O_3 are also plotted for comparison. The total oxidation of toluene to CO_2 and water vapor was confirmed for all catalysts. The toluene oxidation activity of 11Co/CZS/Al_2O_3 was significantly enhanced by the addition of platinum, and despite a smaller platinum loading in the present catalysts, toluene was completely oxidized at a lower temperature of 160 °C compared to that using 5wt%Pt/γ-Al_2O_3 (170 °C). Furthermore, the present 1Pt/11Co/CZS/Al_2O_3 catalyst (complete oxidation of toluene at 160 °C) is more active than 1Pt/CZS/Al_2O_3 (180 °C), indicating the advantage of Co_3O_4 addition to CZS/Al_2O_3. However, the presence of CZS is

indispensable because the oxidation activity of $1Pt/11Co/Al_2O_3$ (210 °C) is smaller than that of $1Pt/11Co/CZS/Al_2O_3$ (160 °C).

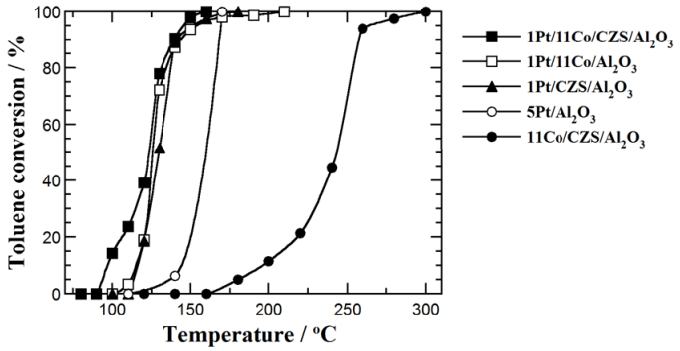

Figure 6. Temperature dependencies of toluene oxidation on the $1wt\%Pt/11wt\%Co_3O_4/16wt\%Ce_{0.62}Zr_{0.20}Sn_{0.18}O_{2.0}/\gamma\text{-}Al_2O_3$ (■), $11wt\%Co_3O_4/16wt\%Ce_{0.62}Zr_{0.20}Sn_{0.18}O_{2.0}/\gamma\text{-}Al_2O_3$ (●), $1wt\%Pt/16wt\%Ce_{0.62}Zr_{0.20}Sn_{0.18}O_{2.0}/\gamma\text{-}Al_2O_3$ (▲), $1wt\%Pt/11wt\%Co_3O_4/\gamma\text{-}Al_2O_3$ (□), and $5wt\%Pt/\gamma\text{-}Al_2O_3$ (○) catalysts

In addition, a supported platinum catalyst was also prepared at 450 °C. The temperature dependencies of toluene oxidation on the $1wt\%Pt/11wt\%Co_3O_4/16wt\%Ce_{0.62}Zr_{0.20}Sn_{0.18}O_{2.0}/\gamma\text{-}Al_2O_3$ catalysts calcined at 450 and 500 °C is shown in Figure 7. Unfortunately, the oxidation activity was not improved. Therefore, the calcination temperature of 500 °C is appropriate for the supported platinum catalyst.

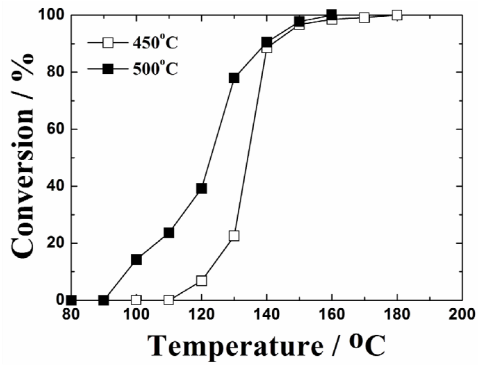

Figure 7. Temperature dependencies of toluene oxidation on the $1wt\%Pt/11wt\%Co_3O_4/16wt\%Ce_{0.62}Zr_{0.20}Sn_{0.18}O_{2.0}/\gamma\text{-}Al_2O_3$ catalysts calcined at 450 °C (□) and 500 °C (■)

To identify the cause for the positive effect of Co_3O_4, TPR spectra of $11Co/CZS/Al_2O_3$ and CZS/Al_2O_3 are measured and their oxygen release behaviors were compared as shown in Figure 8. In the case of CZS/Al_2O_3, the oxygen release peak was observed at 92 °C, while the peak appeared at a lower temperature of 78 °C for $11Co/CZS/Al_2O_3$. Accordingly, the introduction of Co_3O_4 on the CZS/Al_2O_3 support was remarkably effective in enhancing the oxygen supply capability at low temperatures. Furthermore, the total oxygen storage capacity of $11Co/CZS/Al_2O_3$ was 388 μmol O_2 g^{-1}, which was 2.5 times larger than that of CZS/Al_2O_3 (140 μmol O_2 g^{-1}). The increase in the oxygen release and storage abilities was due to the synergistic effects of three redox couples of Ce^{4+}/Ce^{3+}, Sn^{4+}/Sn^{2+}, and Co^{3+}/Co^{2+}, whereby the toluene oxidation was facilitated. As a result, the introduction of Co_3O_4 as a promoter was highly effective in enhancing the catalytic activity.

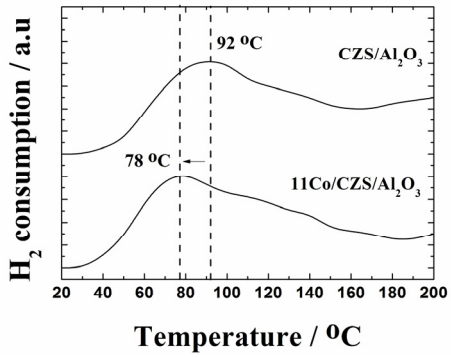

Figure 8. TPR profiles of the 16wt%$Ce_{0.62}Zr_{0.20}Sn_{0.18}O_{2.0}$/γ-$Al_2O_3$ and 11wt%Co_3O_4/16wt%$Ce_{0.62}Zr_{0.20}Sn_{0.18}O_{2.0}$/γ-$Al_2O_3$ catalysts

The oxidation states of Ce, Sn, Co, and Pt in the 1Pt/11Co/CZS/Al_2O_3 catalyst were analyzed by XPS. The XPS results of Ce 3d, Sn 3d, Co 2p, and Pt 4f core-levels are shown in Figure 9. From Figures 9(a) and (b), it is evident that cerium exists both in the trivalent and tetravalent states (Beche et al., 2008; Ma et al., 2009), while tin remains in the tetravalent state and no peaks of the Sn^{2+} species are observed (Kover et al., 1995; Yasuda et al., 2012). In the case of cobalt, the Co 2p peaks in Figure 9(c) are deconvoluted into five peaks. The Co $2p_{3/2}$ and $2p_{3/2}$ peaks can be attributed to the divalent (Co^{2+}: 780.8 and 796.3 eV) and trivalent (Co^{3+}: 779.5 and 794.5 eV) oxidation states, and the broad one at 786.0 eV corresponds to a satellite peak of Co^{2+} (Liotta et al., 2006; Xiao et al., 2008). These are the typical results for Co_3O_4 (Liotta et al., 2009). The Pt 4f peaks are shown in Figure 9(d). Although the Pt $4f_{5/2}$ peak at 74.4 eV overlaps that of Al 2p in the present case, the small Pt $4f_{7/2}$ peak is clearly observed at 70.9 eV, which can be attributed to the metallic platinum (Pt^0) (Zhang et al., 2003).

Taking into account of the catalysis, TPR, and XPS results, the high oxidation activity of toluene observed in 1Pt/11Co/CZS/Al_2O_3 can be attributed to a concerted effect of Pt, Co_3O_4, and $Ce_{0.62}Zr_{0.20}Sn_{0.18}O_{2.0}$ supported on γ-Al_2O_3. The readily reducible Co_3O_4 and $Ce_{0.62}Zr_{0.20}Sn_{0.18}O_{2.0}$ contribute to the supplementation of active oxygen species from the catalyst bulk, and the oxygen reacts with toluene at the interface of three Pt, Co_3O_4, and $Ce_{0.62}Zr_{0.20}Sn_{0.18}O_{2.0}$ phases. As a result, complete toluene oxidation was realized using the present 1Pt/11Co/CZS/Al_2O_3 catalyst at a temperature of 160 °C which is lower than that of 5wt%Pt/γ-Al_2O_3 (170 °C), in spite of a smaller amount of platinum.

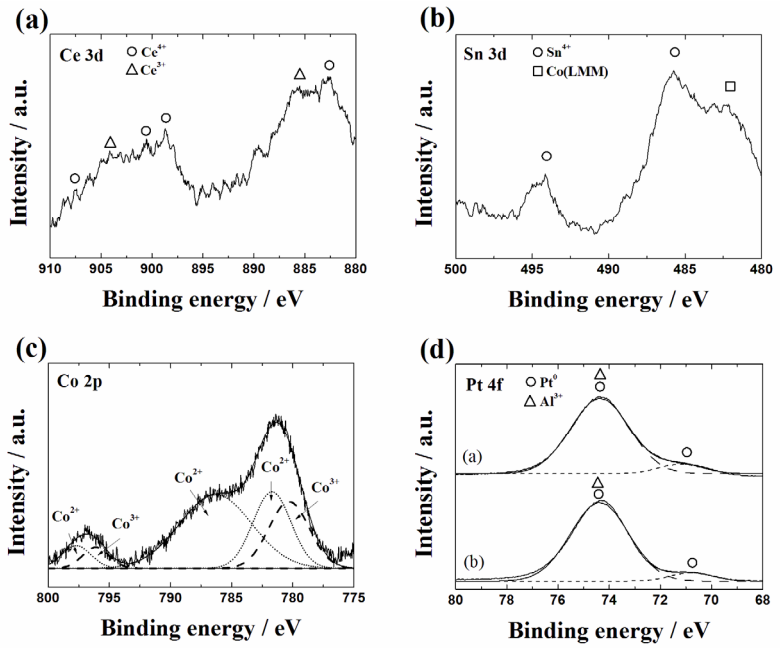

Figure 9. XPS results of the 1wt%Pt/11wt%Co_3O_4/16wt%$Ce_{0.62}Zr_{0.20}Sn_{0.18}O_{2.0}$/γ-$Al_2O_3$ catalyst : (a) Ce 3d, (b) Sn 3d, (c) Co 2p, and (d) Pt 4f core-levels

4. Conclusions

Co_3O_4/CeO_2-ZrO_2-SnO_2/γ-Al_2O_3 and $Pt/Co_3O_4/CeO_2$-ZrO_2-SnO_2/γ-Al_2O_3 catalysts were successfully prepared by the conventional co-precipitation and impregnation methods. The catalytic tests for toluene oxidation on these materials showed that addition of Co_3O_4 to a Pt/CeO_2-ZrO_2-SnO_2/γ-Al_2O_3 catalyst was significantly effective in decreasing the amount of platinum without significant reduction in the activity. In fact, complete oxidation of toluene was realized using the 1wt%Pt/11wt%Co_3O_4/16wt%$Ce_{0.62}Zr_{0.20}Sn_{0.18}O_{2.0}/\gamma$-$Al_2O_3$ catalyst at 160 °C, which was lower than that using the 5wt%Pt/γ-Al_2O_3 catalyst (170 °C). Since the oxidation activities of 1wt%Pt/16wt%$Ce_{0.62}Zr_{0.20}Sn_{0.18}O_{2.00}/\gamma$-$Al_2O_3$ and 1wt%Pt/11wt%Co_3O_4/γ-Al_2O_3 were lower than that of 1wt%Pt/11wt%Co_3O_4/16wt%$Ce_{0.62}Zr_{0.20}Sn_{0.18}O_{2.0}/\gamma$-$Al_2O_3$, the cause for the high toluene oxidation activity observed in the 1wt%Pt/11wt%Co_3O_4/16wt%$Ce_{0.62}Zr_{0.20}Sn_{0.18}O_{2.0}/\gamma$-$Al_2O_3$ catalyst can be attributed to the concerted effect of Pt, Co_3O_4, and $Ce_{0.62}Zr_{0.20}Sn_{0.18}O_{2.0}$ supported on γ-Al_2O_3.

Acknowledgements

This study was partially supported by the Industrial Technology Research Grant Program ’08 (Project ID: 08B42001a) from the New Energy and Industrial Technology Development Organization (NEDO) of Japan, and the Environment Research and Technology Development Fund (B-0907) of the Ministry of the Environment, Japan.

References

Atkinson, R., & Arey, J. (2003). Atmospheric degradation of volatile organic compounds. *Chemical Reviews, 103*, 4605-4638. http://dx.doi.org/10.1021/cr0206420

Beche, E., Charvin, P., Perarnau, D., Abanades, S., & Flamant, G. (2008). Ce 3d XPS investigation of cerium oxides and mixed cerium oxide ($Ce_xTi_yO_z$). *Surface and Interface Analysis, 40*, 264-267. http://dx.doi.org/10.1002/sia.2686

Chianelli, R. R., Berhault, G., & Torres, B. (2009). Unsupported transition metal sulfide catalysts: 100 years of science and application. *Catalysis Today, 147*, 275-286. http://dx.doi.org/10.1016/j.cattod.2008.09.041

Einaga, H., Futamura, S., & Ibusuki, T. (2002). Heterogeneous photocatalytic oxidation of benzene, toluene, cyclohexene and cyclohexane in humidified air: comparison of decomposition behavior on photoirradiated TiO_2 catalyst. *Applied Catalysis B: Environmental, 38*, 215-225. http://dx.doi.org/10.1016/S0926-3373(02)00056-5

Hamins, A., & Seshadri, K. (1987). The structure of diffusion flames burning pure, binary, and ternary solutions of methanol heptane and toluene. *Combustion and Flame, 68*, 295-307. http://dx.doi.org/10.1016/0010-2180(87)90006-X

Harling, A. M., Glover, D. J., Whitehead, J. C., & Zhang, K. (2009). The role of ozone in the plasma-catalytic destruction of environmental pollutants. *Applied Catalysis B: Environmental, 90*, 157-161. http://dx.doi.org/10.1016/j.apcatb.2009.03.005

Hauxell, F., & Ottewill, R. H. (1968). The adsorption of toluene vapor on water surfaces. *Journal of Colloid and Interface Science, 28*, 514-521. http://dx.doi.org/10.1016/0021-9797(68)90084-2

Imanaka, N., Masui, T., Minami, K., & Koyabu, K. (2005). Promotion of low-temperature reduction behavior of the CeO_2-ZrO_2-Bi_2O_3 solid solution by addition of silver. *Chemistry Materials, 17*, 6511-6513. http://dx.doi.org/10.1021/cm0519380

Imanaka, N., Masui, T., Koyabu, K., Minami, K., & Egawa, T. (2007). Significant low-temperature redox activity of $Ce_{0.64}Zr_{0.16}Bi_{0.20}O_{1.90}$ supported on γ-Al_2O_3. *Advanced Materials, 19*, 1608-1611. http://dx.doi.org/10.1002/adma.200502741

Imanaka, N., Masui, T., Terada, A., & Imadzu, H. (2008). Complete oxidation of ethylene at temperatures below 100 ^oC over a $Pt/Ce_{0.64}Zr_{0.16}Bi_{0.20}O_{1.90}/\gamma$-$Al_2O_3$ catalyst. *Chemistry Letters, 37*, 42-43. http://dx.doi.org/10.1246/cl.2008.42

Imanaka, N., & Masui, T. (2009). Advanced materials for environmental catalysts. *Chemical Record, 9*, 40-50. http://dx.doi.org/10.1002/tcr.20167

Imanaka, N., Masui, T., & Yasuda, K. (2011). Environmental catalysts for complete oxidatioin of volatile organic compounds and methane. *Chemistry Letters, 40*, 780-785. http://dx.doi.org/10.1246/cl.2011.780

Kover, L., Kovacs, Zs., Sanjines, R., Mretti, G., Cserny, I., Margaritondo, G., … Adachi, H. (1995). Electronic structure of tin oxides: High-resolution study of XPS and auger spectra. *Surface and Interface Analysis, 23*,

461-466. http://dx.doi.org/10.1002/sia.740230705

Lamonier, J. F., Boutoundou, A. B., Gennequin, C., Perez-Zurita, M. J., Siffert, S., & Aboukais, A. (2007). Catalytic removal of toluene in air over Co-Mn-Al nano-oxides synthesized by hydrotalcite route. *Catalysis Letters, 118*, 165-172. http://dx.doi.org/10.1007/s10562-007-9196-4

Liotta, L. F., Di Carlo, G., Pantaleo, G., Venezia, A. M., & Danello, G. (2006). Co_3O_4/CeO_2 composite oxides for methane emissions abatement: Relationship between Co_3O_4-CeO_2 interaction and catalytic activity. *Applied Catalysis B: Environmental, 66*, 217-227. http://dx.doi.org/10.1016/j.apcatb.2006.03.018

Liotta, L. F., Ousmane, M., Carlo, G. D., Pantaleo, G., Deganello, G., Boreave, A., & Fendler, A. G. (2009). Catalytic removal of toluene over Co_3O_4-CeO_2 mixed oxide catalysts: Comparison with Pt/Al_2O_3. *Catalysis Letters, 127*, 270-276. http://dx.doi.org/ 10.1007/s10562-008-9640-0

Ma, Y., Ge, Q., Li, W., & Xu, H. (2009). Methanol synthesis from sulfur-containing syngas over Pd/CeO_2 catalyst. *Applied Catalysis B: Environmental, 90*, 99-104. http://dx.doi.org/ 10.1016/j.apcatb.2009.02.020

Masui, T., Minami, K., Koyabu, K., & Imanaka, N. (2006). Synthesis and characterisation of new promoters based on CeO_2-ZrO_2-Bi_2O_3 for automotive exhaust catalysts. *Catalysis Today, 117*, 187-192. http://dx.doi.org/ 10.1016/j.cattod.2006.05.015

Masui, T., Koyabu, K., Minami, K., Egawa, T., & Imanaka, N. (2007). Low-temperature redox activity of $Ce_{0.64}Zr_{0.16}Bi_{0.20}O_{1.90}/\gamma$-$Al_2O_3$ and $Ag/Ce_{0.64}Zr_{0.16}Bi_{0.20}O_{1.90}/\gamma$-$Al_2O_3$ catalysts. *The Journal of Physical Chemistry C, 111*, 13892-13897. http://dx.doi.org/ 10.1021/jp072634z

Masui, T., Imadzu, H., Mastuyama, N., & Imanaka, N. (2010). Total oxidation of toluene on Pt/CeO_2-ZrO_2-Bi_2O_3/γ-Al_2O_3 catalysts prepared in the presence of polyvinyl pyrrolidone. *Journal of Hazardous Materials, 176*, 1106-1109. http://dx.doi.org/10.1016/j.jhazmat.2009.11.108

Minami, K., Masui, T., Imanaka, N., Dai, L., & Pacaud, B. (2006). Redox behavior of CeO_2-ZrO_2-Bi_2O_3 and CeO_2-ZrO_2-Y_2O_3 solid solutions at moderate temperatures. *Journal of Alloys and Compounds, 408-412*, 1132-1135. http://dx.doi.org/10.1016/j.jallcom.2004.12.141

Pedrosa, A. M. G., Souza, M. J. B., Fernandes, J. D. G., Melo, D. M. A., & Araujo, A. S. (2003). *n*-Heptane oxidation over Co_3O_4-CeO_2 catalyst. *Reaction Kinetics and Catalysis Letters, 79*, 391-396. http://dx.doi.org/10.1023/A:1024562924637

Ryerson, T. B., Trainer, M., Holloway, J. S., Parrish, D. D., Huey, L. G., Sueper, D. T., … Fehsenfled, F. C. (2001). Observations of ozone formation in power plant plumes and implication for ozone control strategies. *Science, 292*, 719-723. http://dx.doi.org/10.1126/science.1058113

Rybak, P., Tomaszewska, B., Machocki, A., Grzegorczyk, W., & Denis, A. (2011). Conversion of ethanol over supported cobalt oxide catalysts. *Catalsis Today, 176*, 14-20. http://dx.doi.org/10.1016/j.cattod.2011.06.015

Sungkono, I. E., Kameyama, H., & Koya, T. (1997). Development of catalytic combustion technology of VOC materials by anodic oxidation catalyst. *Applied Surface Science, 121/122*, 425-428. http://dx.doi.org/10.1016/S0169-4332(97)00352-8

Spivey, J. J. (1987). Complete catalytic oxidation of volatile organics. *Industrial and Engineering Chemistry Research, 26*, 2165-2180. http://dx.doi.org/10.1021/ie00071a001

Saqer, S. M., Kondarides, D. I., & Verykios, X. E. (2009). Catalytic activity of supported platinum and metal oxide catalysts for toluene oxidation. *Topics in Catalysis, 52*, 517-527. http://dx.doi.org/10.1007/s11244-009-9182-8

Wyrwalski, F., Giraudon, J. M., & Lamonier, J. F. (2010). Synergistic coupling of the redox properties of supports and cobalt oxide Co_3O_4 for the complete oxidation of volatile organic compounds. *Catalysis Letters, 137*, 141-149. http://dx.doi.org/10.1007/s10562-010-0356-6

Xiao, Q., Zhang, J., Xiao, C., & Tan, X. (2008). Photocatalytic degradation of methylene blue over Co_3O_4/Bi_2WO_6 composite under visible light irradiation. *Catalysis Communications, 9*, 1247-1253. http://dx.doi.org/10.1016/j.catcom.2007.11.011

Yasuda, K., Yoshimura, A., Katsuma, A., Masui, T., & Imanaka, N. (2012). Low-temperature complete combustion of volatile organic compounds over novel Pt/CeO_2-ZrO_2-SnO_2/γ-Al_2O_3 catalysts. *Bulletin of the Chemical Society of Japan, 85*, 522-526. http://dx.doi.org/10.1246/bcsj.20110382

Zhang, X., & Chan, K. (2003). Water-in-oil microemulsion synthesis of platinum-ruthenium nanoparticles their characterization and electrocatalytic properties. *Chemistry of Materials, 15*, 451-459. http://dx.doi.org/10.1021/cm0203868